FOREST FEATURE LIDAR SLAM (F^2-LSLAM) AND INTEGRATED SCAN SIMULTANEOUS TRAJECTORY ENHANCEMENT AND MAPPING (IS^2-TEAM) FOR ACCURATE FOREST INVENTORY USING BACKPACK SYSTEMS

C. Zhao [1], T. Zhou [1], S. Fei [2], and A. Habib [1] *

[1] Lyles School of Civil Engineering, Purdue University, West Lafayette, IN 47907, USA - (zhao1259, zhou732, ahabib)@purdue.edu

[2] Forestry and Natural Resources, Purdue University, West Lafayette, IN 47907, USA - sfei@purdue.edu

KEY WORDS: LiDAR, Backpack MMS, UAV MMS, SLAM, GNSS/INS trajectory enhancement, forest inventory

ABSTRACT:

Under-canopy mapping is desired to derive critical forest biometrics, such as diameter at breast height (DBH), merchantable height, and debris volume. The main challenge of such under-canopy mapping is the intermittent access to the global navigation satellite system (GNSS) signal, which is crucial to deriving accurately georeferenced mapping products. In this study, we propose two frameworks – Forest Feature LiDAR Simultaneous Localization and Mapping (F^2-LSLAM) and Integrated Scan Simultaneous Trajectory Enhancement and mapping (IS^2-TEAM) – for 3D LiDAR unit mounted on backpack systems to achieve accurate forest inventory. In the F^2-LSLAM strategy, ground/tree trunk features are extracted from individual LiDAR scans. On the other hand, when trajectory information provided by navigation sensors is available, these semantic features are derived from LiDAR points within several scans (i.e., integrated scan) for the IS^2-TEAM strategy. Then, local/global least squares adjustment (LSA) using derived features is performed to register LiDAR scans to a common reference frame for both strategies. To evaluate the performance of the proposed strategies, three in-house developed backpack systems with varying specifications were used to collect data in complicated forest environments. Through the comparison with point clouds acquired by a commercial backpack LiDAR system, the proposed frameworks are capable of generating point clouds with satisfactory intra-dataset alignment quality (in the range of 2-4 cm) for all backpack systems in natural forest areas with relatively flat terrain. However, for more challenging areas with dense undergrowth vegetation and/or large height differences, F^2-LSLAM framework cannot extract sufficient features, while IS^2-TEAM still exhibits good performance.

1. INTRODUCTION

Accurate forest inventory provides substantial information, which is essential for the management of long-term sustainability of forest ecosystems (Kangas and Maltamo, 2006). Traditional forest inventory is conducted manually, which is labor-intensive, costly, and time-consuming. To improve the efficiency, remote/proximal sensing techniques – e.g., LiDAR and photogrammetric mapping using above-canopy and under-canopy platforms – have been adopted as alternative approaches for automated forest inventory at various scales. During the past decade, researchers utilized imagery/LiDAR data acquired by crewed aerial systems to estimate inventory attributes such as tree height, crown dimension, stem map, and timber volume (Goodbody et al., 2019; Khosravipour et al., 2014). Nowadays, uncrewed aerial vehicles (UAVs) have attracted the attention of the forestry research community due to their low cost, ease of deployment, rapid acquisition, and ability to deliver fine spatial/temporal resolution products. For instance, forest biometrics were derived using orthophotos and point clouds generated from UAV images (Miller et al., 2021), while UAV LiDAR data have been adopted for segmenting individual trees (Corte et al., 2020). Nevertheless, with above-canopy flights, the ability of camera/LiDAR to map under-canopy features is limited by tree density and leaf cover. Detailed under-canopy mapping, which is necessary for deriving accurate estimates of critical forest biometrics such as diameter at breast height (DBH) and merchantable height, is not always guaranteed. In these scenarios, under-canopy LiDAR mapping is preferred (Hyyppä et al., 2020).

Under-canopy LiDAR mapping platforms can be categorized into stationary terrestrial laser scanners (TLS) and mobile LiDAR systems. Although the former provide high-quality data for deriving forest structural metrics at the stand-level (Barbeito et al., 2017), data acquisition using TLS is not scalable since large field surveys and point cloud registration are time-consuming. On the other hand, mobile LiDAR systems can maneuver under-canopy to obtain relatively larger spatial coverage while minimizing occlusions. The majority of mobile LiDAR systems rely on an onboard integrated global navigation satellite system/inertial navigation system (GNSS/INS) unit – i.e., direct georeferencing – to provide the position and orientation information for point cloud generation. The main challenge of such under-canopy mapping is the intermittent access to the GNSS signal, which is crucial to deriving accurately georeferenced mapping products from the onboard sensors.

To mitigate the impact of GNSS-challenging environments on the derived LiDAR point clouds, trajectory enhancement strategies were adopted. For instance, Kukko et al. (2017) derived the centroids of tree trunks from LiDAR point clouds reconstructed every few seconds. By minimizing the discrepancy among conjugate centroids, GNSS/INS-derived trajectory was refined. Based on the same concept, Zhou et al. (2023) employed tree trunk and terrain patch features for trajectory enhancement. The major limitation of such strategies is the requirement of an initial GNSS/INS trajectory with reasonable accuracy.

Advances in Simultaneous Localization and Mapping (SLAM) offer an alternative to direct georeferencing in GNSS-denied/challenging scenarios. Several studies have been conducted to evaluate the performance of LiDAR SLAM in forest environments. Tang et al. (2015) investigated a LiDAR-inertial SLAM strategy. By minimizing the discrepancy between conjugate 2D stem locations from different timestamps while considering the measurements from the inertial measurement unit (IMU), an extended Kalman filter (EKF) was adopted to derive the trajectory. Pierzchała et al. (2018) developed an Iterative Closest Point (ICP)-based SLAM algorithm to estimate the relative transformation between successive LiDAR scans. This process was followed by loop closure and optimization steps to

* Corresponding author

derive the final trajectory. Chen et al. (2020) proposed a Semantic LiDAR Odometry and Mapping (SLOAM) algorithm. In SLOAM, trees and ground features were derived through a hybrid deep learning and morphological based segmentation process from individual LiDAR scans (i.e., LiDAR points from a full revolution of the laser beam assembly). Odometry and mapping threads were conducted to estimate the transformation parameters between successive scans and register all scans to a common reference frame, respectively. In their process, the attributes related to the extracted semantic features, e.g., the diameter of the trees, could be provided. However, the lack of long-term optimization in their approach will result in accumulated errors.

Recently, commercial under-canopy mobile 3D LiDAR systems integrated with SLAM techniques have become available. Several studies investigated the performance of these commercial systems, including (i) the backpack/handheld LiDAR systems developed by Emesent Hovermap Ltd. (Australia) (Hartley et al., 2022), (ii) the handheld LiDAR systems developed by GeoSLAM Ltd. (UK) (Sofia et al., 2021), and (iii) the backpack LiDAR systems developed by Digital Green Valley Technology Ltd. (China) (Xie et al., 2022). These systems have shown promising results for forest inventory applications. However, they are limited in terms of their ability to provide critical semantic features for forest inventory applications during the SLAM process.

This study proposes two frameworks – Forest Feature LiDAR SLAM (F^2-LSLAM) and Integrated Scan Simultaneous Trajectory Enhancement and mapping (IS^2-TEAM) – using a single, non-rotating 3D LiDAR mounted on backpack systems for accurate forest inventory. More specifically, F^2-LSLAM consists of odometry and mapping threads. In the odometry thread, semantic features – tree trunks and ground – are extracted from individual scans. The mapping thread registers LiDAR scans to a common reference frame through local/global LSA using extracted features. As for IS^2-TEAM, trajectory information provided by the onboard navigation units is required and used to generate LiDAR points from several scans (i.e., an integrated scan). Thus, feature extraction is performed on the integrated scans where the definition of features is more complete. Then, the same mapping thread of F^2-LSLAM is utilized to register all integrated scans.

2. BACKPACK SYSTEMS AND DATASETS DESCRIPTION

This section begins with an introduction to the backpack systems and sensors utilized in this study. Then, the acquired datasets used for evaluating the proposed frameworks are described.

2.1 Backpack Mobile Mapping Systems

In this study, three in-house developed backpack mobile mapping systems with different specifications – i.e., the number of laser beams and coverage of a single scan – are used for evaluation of two proposed frameworks. For each system, a 3D LiDAR unit is installed with the rotational axis of its laser beam assembly 45° – 55° away from the vertical direction. Such design ensures the capability to capture the upper canopy for forest inventory. The first backpack system – *BP-HDL32* – comprises a Velodyne HDL-32E LiDAR, two Sony α6000 cameras, and a NovAtel PwrPak7-E2 GNSS/INS unit, as shown in Figure 1a. The second backpack system – *BP-VLP16* – carries a Velodyne VLP-16 LiDAR and a NovAtel PwrPak7-E1 GNSS/INS unit, as shown in Figure 1b. The third backpack system – *BP-VLP16HR* – carries a Velodyne VLP-16 Hi-Res LiDAR, a Sony α7R II camera, and a NovAtel SPAN-CPT GNSS/INS unit, as shown in Figure 1c. The specifications of used LiDAR and GNSS/INS units are listed in Table 1. For the 3D LiDAR units on these three systems, the number of revolutions per minute (i.e., RPM setting) is set to 600, resulting in a LiDAR scan duration of 0.1 seconds. It is worth mentioning that the onboard cameras are not used in this study.

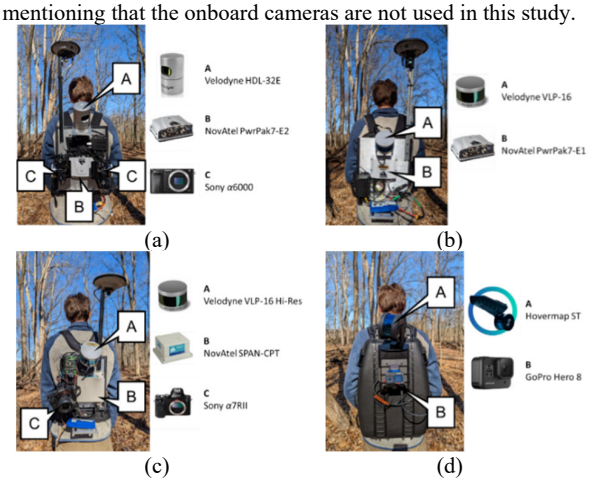

Figure 1. The backpack mobile mapping systems and onboard sensors used in this study: the in-house developed (a) *BP-HDL32*, (b) *BP-VLP16*, and (c) *BP-VLP16HR* systems, as well as (d) off-the-shelf Hovermap Backpack system.

System	*BP-HDL32*	*BP-VLP16*	*BP-VLP16HR*
LiDAR Specifications			
# of laser beams	32	16	16
Horizontal FOV	360°	360°	360°
Vertical FOV (angle range from sensor's horizon)	41.33° (-30.67° to +10.67°)	30 ° (-15° to +15°)	20 ° (-10° to +10°)
Pulse per second	~695,000	~300,000	~300,000
GNSS/INS Specifications			
IMU data rate	200 Hz	200 Hz	100 Hz
Positional accuracy *	1-2 cm	1-2 cm	1-2 cm
Roll/pitch accuracy *	0.005°	0.009°	0.008°
Heading accuracy *	0.010°	0.044°	0.026°

* After GNSS/INS post-processing in open sky conditions

Table 1. Specifications of LiDAR and GNSS/INS units mounted on the in-house developed backpack systems.

In addition to the three in-house developed backpack systems, this study also includes a commercial backpack LiDAR system developed by Emesent Hovermap Ltd. (hereafter denoted as *BP-HM*) for comparison purposes. This system comprises a Hovermap ST – i.e., SLAM-based LiDAR unit – and a GoPro Hero 8, as shown in Figure 1d. During data acquisition, the 3D LiDAR unit mounted on the Hovermap ST rotates, providing an angular field of view (FOV) of 360° by 290°. The *BP-HM* captures approximately 300,000 points per second (similar to *BP-VLP16* and *BP-VLP16HR* systems). The provided SLAM-based post-processing software allows for a mapping accuracy of 2 cm.

2.2 Datasets Description

The study sites used for this research are at a natural forest within Martell Forest – a research forest owned and managed by Purdue University, in West Lafayette, Indiana, USA, as depicted in Figure 2a. In this natural forest, black oak, white oak, yellow poplar, ash, basswood, and sugar maple are the major species. There is a significant amount of large and mature timber, but also young and more vigorous small sawtimber resulting from a large influx of regeneration at some point in the past. Shrubby species – mainly bladdernut – make up a large portion of the understory vegetation. The average DBH is 29.7 cm for those trees whose diameter exceeds 7.6 cm.

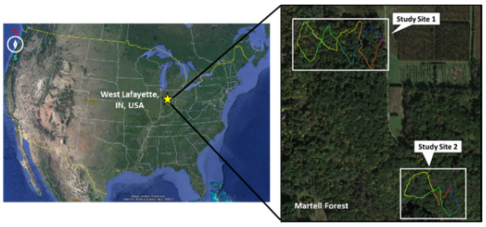

(a)

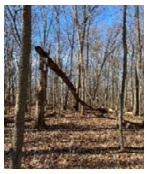

(b)

(c)

Figure 2. (a) Location of the study sites and the sample trajectory (colored by time) of the collected backpack datasets; terrestrial images captured on the same date of data acquisition for (b) study site 1 under leaf-off condition and (c) study site 2 under leaf-on condition.

For study site 1 with relatively flat terrain, four backpack datasets were collected following the same route using the *BP-HDL32*, *BP-VLP16*, *BP-VLP16HR*, and *BP-HM* systems on March 2nd, 2023 under leaf-off condition. Each mission lasted around 13 minutes, covering an area of approximately 4 ha with an 800 m long trajectory. The mission route started and ended at the same location, allowing for a qualitative assessment of the trajectory's alignment from the beginning and end. Additionally, a UAV LiDAR dataset covering the study site acquired on March 3rd, 2022 was used as a reference point cloud. The UAV was flown at 60 m height above ground, providing point cloud with an expected accuracy at the nadir position in the range of 7-8 cm.

As for study site 2, this area is densely populated with low vegetation, and the elevation difference is up to 20 m, as shown in Figure 2c. Two backpack datasets following the same track were collected on May 31st, 2023 under leaf-on condition using *BP-VLP16HR* and *BP-HM* systems. Each mission lasted around 12 minutes, covering an area of approximately 1 ha with a 500 m long trajectory. This study site is more challenging considering the dense undergrowth vegetation and height difference when compared to study site 1.

3. F²-LSLAM AND IS²-TEAM FRAMEWORKS

LiDAR point cloud reconstruction is based on the point positioning equation, as graphically illustrated in Figure 3. Raw LiDAR data are used to derive the position of the laser beam footprint at an object point I captured at firing time t relative to the lu frame, $r_I^{lu(t)}$. To compute the 3D coordinates, r_I^m, of the object point I in a given reference frame – i.e., the mapping frame (m), the position and orientation, $r_{lu(t)}^m/R_{lu(t)}^m$, of the laser unit frame at time t relative to the mapping frame need to be established in the F²-LSLAM and IS²-TEAM processes.

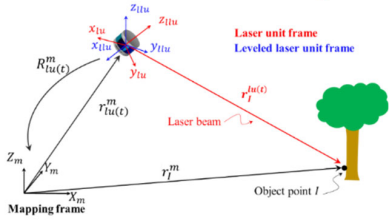

Figure 3. Parameters and coordinate systems involved in the point positioning equation for LiDAR reconstruction.

The proposed F²-LSLAM framework includes odometry and mapping threads, while the IS²-TEAM framework consists of feature extraction process and the same mapping thread, as shown in Figure 4. The odometry thread of F²-LSLAM extracts ground/tree features from each LiDAR scan and estimates the relative transformation between successive scans. On the other hand, the IS²-TEAM framework employs trajectory information provided by the onboard navigation sensors (GNSS/INS unit in this study) for more reliable feature extraction. Specifically, although the absolute accuracy of the derived trajectory is negatively affected by GNSS signal outages, the relative position and orientation information in a short period (within a few seconds) is still reasonable and used to generate the integrated scan. Then, feature extraction is performed on the integrated scans where the definition of features is more complete. The mapping thread performs local and global LSA using extracted semantic features to register individual/integrated LiDAR scans to a common reference frame and refine pose parameters derived from the odometry thread or provided by the trajectory. Moreover, the proposed strategies also support the incorporation of reference point clouds in the process.

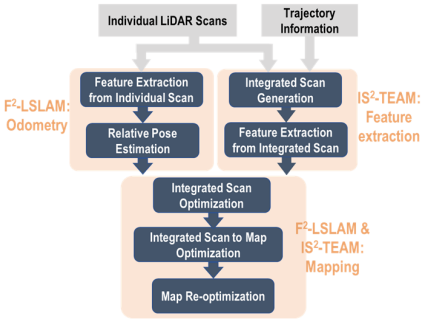

Figure 4. Proposed F²-LSLAM and IS²-TEAM frameworks.

3.1 Odometry Thread of F²-LSLAM

In this process, feature extraction is conducted through morphological strategies from individual scans (a sample LiDAR scan from the *BP-HDL32* system is shown in Figure 5a), starting with segmenting ground areas followed by clustering individual tree trunks. To achieve this, the point cloud needs to be leveled so that LiDAR points representing the ground can be extracted based on the elevation while the points that constitute cylinders/lines perpendicular to the ground could be potential tree features. In this study, a leveled laser unit frame (llu) is introduced to address the challenges caused by the unleveled installation of the used LiDAR unit. The origin of llu frame is the same as lu frame, and the Z axis of llu frame is along the plumb line (as shown in Figure 3).

The feature extraction process for a LiDAR scan is conducted in four steps. Firstly, connected consecutive LiDAR points corresponding to the same object captured by a given laser beam are grouped as segments according to the similarity of their range measurements. Then, by assuming the ground is relatively smooth and horizontal in a local neighborhood, some ground portions are extracted by clustering the segments from neighboring scan lines. An initial ground model is derived from these portions to level the LiDAR scan (i.e., transform the LiDAR scan to the llu frame). Once the scan is leveled, a complete representation of the ground is extracted by finding the LiDAR segments with the lowest elevation in a local neighborhood. Lastly, the remaining non-ground segments that constitute vertical cylinders/lines in the llu frame are identified as tree trunk features. The derived ground and tree trunk features from the sample LiDAR scan is shown in Figure 5b.

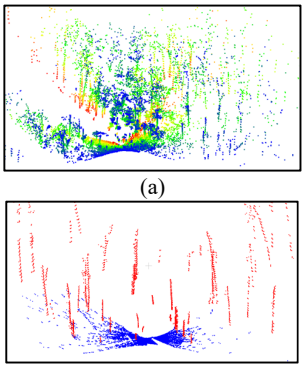

(a)

(b)

Figure 5. (a) Sample LiDAR scan from the *BP-HDL32* system (colored by laser beam ID) and (b) extracted ground and tree trunk features (colored in blue and red, respectively).

Based on the extracted features, relative pose estimation between successive LiDAR scans is conducted in the odometry thread. Since a single ground model is estimated from each scan, they are directly matched and used to derive the $d\omega$, $d\phi$, and dZ components of the pose parameters in question. Then, a 2D nearest neighbor search is used to match tree trunk features from the two scans. By minimizing the sum of squared distances between 2D locations of matched tree trunks, $dX, dY,$ and $d\kappa$ components are solved through a linear LSA process.

The performance of relative pose estimation relies on the extracted features from LiDAR scans. Failure to extract sufficient features from the scans will affect its performance. To overcome this challenge, trajectory information provided by the GNSS/INS unit can be used in the process. Specifically, relative pose parameters are derived from the trajectory information considering the short duration between successive scans (i.e., ~0.1 seconds for the used systems).

3.2 Feature Extraction of IS^2-TEAM

In areas with dense vegetation or steep terrain, extracting features from an individual LiDAR scan can be difficult. To address these challenges, extracting features from LiDAR points over a longer duration is preferred. Assuming that the relative transformation derived from the GNSS/INS trajectory is of reasonable accuracy, integrated scans consisting of a specific number of individual scans are derived in this study, as shown in Figure 6a.

The feature extraction process starts by partitioning the integrated scan into a grid using a pre-defined cell size. The lowest point in each cell is identified as a potential ground point (PGP). A region-growing process is performed starting from the PGP with the shortest range measurement to identify PGPs with consistent height information, which are denoted as initial ground points. Unclassified PGPs with high planarity values (calculated from neighboring PGPs), are labelled as seed points for an additional round of region-growing. Finally, the results from above region-growing steps are combined as the augmented ground points.

In the next step, a Triangulated Irregular Network (TIN)-based interpolation is used to generate a DTM. The augmented ground points are used to create a TIN, and the height values of the DTM cells are interpolated using the TIN. The classification of bare earth (BE) and above-ground (AG) points is then performed. Points that have a height difference below a threshold compared to the corresponding DTM cell are classified as BE points, while the rest are classified as AG points.

Tree trunk feature extraction is performed on the AG points. First, the heights of the AG points are normalized using the DTM. The lower portion of the normalized AG points, which is assumed to represent the tree trunk, is isolated based on user-defined height thresholds. A tree detection and localization approach proposed by Lin et al. (2021a) is then applied to segment the isolated AG points based on estimated tree locations. Criteria based on the number of points and height range are used to filter out unreliable segments. A cylinder model is fitted to the surviving tree trunk features to eliminate points with large residuals. The results of the ground and tree trunk feature extraction are shown in Figure 6b.

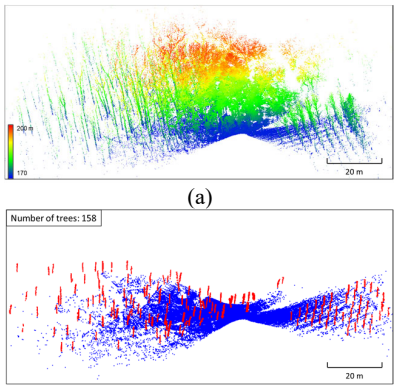

(a)

(b)

Figure 6. (a) Sample integrated scan consisting of 100 individual scans from the *BP-VLP16HR* system (colored by height) and (b) extracted ground/tree trunk features (colored in blue and red, respectively).

3.3 Mapping Thread of F^2-LSLAM and IS^2-TEAM

Once semantic features from each individual scan or integrated scan are extracted, all individual/integrated scans will be sequentially aligned relative to a common/mapping frame through three layers of optimization processes, namely: integrated scan optimization, integrated scan to map optimization, and map re-optimization. The involved procedures will be presented in this subsection.

Integrated scan optimization

In the F^2-LSLAM framework, successive LiDAR scans will be registered to a local reference frame named integrated scan coordinate system (i-s) using the relative pose parameters estimated from the odometry thread. Conjugate tree trunk features from the involved scans are also identified. As for the IS^2-TEAM strategy, the integrated scan has already been generated using the provided GNSS/INS trajectory information. Meanwhile, tree trunk features and ground points within the integrated scan have been derived.

In this process, pose parameters relative to the i-s frame are refined through an optimization process that uses tree trunk and ground patch features. While the matched/derived tree trunk features are modeled as cylinders, ground patches are extracted from the ground points using regularly spaced 2D seed points and modeled as planes. For a seed point, a 2D square region is defined with a given size (e.g., 1 m) – ground points within this region are identified and form a ground patch. A non-linear LSA is conducted to solve for the pose parameters of involved scans and the parametric models of used features (i.e., cylinder and planar features for tree trunk features and ground patches) through the minimization of the sum of squared normal distances of feature points to respective models. Figure 7 shows the established tree trunk features and ground patches from a sample integrated scan before and after the optimization, where the alignment of tree trunk features improves significantly through the optimization.

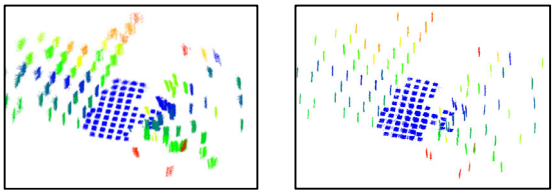

(a) (b)

Figure 7. Sample results from the integrated scan optimization procedure with 100 scans: extracted tree trunk features (colored by feature ID) and ground patches (colored in blue) (a) before and (b) after the optimization process.

Integrated scan to map optimization

The integrated scan to map optimization is performed to determine the transformation from the *i-s* frame to the mapping frame ($r^m_{i\text{-}s}/R^m_{i\text{-}s}$). A map could be created by the first integrated scan, where each tree trunk feature initializes a map tree, and ground points from this integrated scan initialize the ground map. Then, subsequent integrated scans are sequentially aligned to the map. In case a reference point cloud in a known coordinate system is available, it could be employed to initialize the map. By doing so, products of the proposed frameworks are defined in the same coordinate system, facilitating multi-system/temporal evaluation. The reference point cloud also provides additional control information to reduce drifts. In this study, a DTM and tree locations are derived from a reference point cloud. The former will be used as the ground map, and each detected tree location initializes a map tree.

Integrated scan to map optimization is achieved by aligning the features from integrated scan to the map. For tree trunk features in the current integrated scans, the corresponding map trees are identified through nearest neighbor search. For each ground point, its corresponding control plane is derived from the ground map. Figure 8a shows the features that will be used in the optimization and the zoom-in window shows the initial alignment between matched tree trunk features. In the next step, the $r^m_{i\text{-}s}/R^m_{i\text{-}s}$ in question are refined through a non-linear LSA process by minimizing the discrepancy between the matched tree trunk features as well as ground point to the corresponding control plane derived from current integrated scan and map. Figure 8b shows the alignment of matched features after optimization, where the discrepancies between the matched tree objects and map trees are minimized. After optimization, the ground and tree trunk features from the current integrated scan are used to update the map.

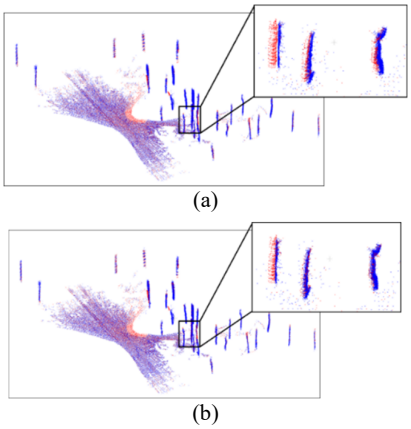

(a)

(b)

Figure 8. Used tree trunk features and ground points (a) before and (b) after optimization (points from the current integrated scan and map are colored in red and blue, respectively).

Map re-optimization

As integrated scans are added to the map, errors will accumulate over time. To reduce drifts in the map, frequent long-term optimization that simultaneously refines pose and feature parameters – i.e., map re-optimization – is conducted. Similar to integrated scan optimization, map re-optimization is achieved by minimizing the discrepancies among conjugate features. For ground patches, the same approach used in the integrated scan optimization is adopted to extract them from the ground points in the map. Figure 9a shows the used map trees and ground patches in the map re-optimization. Next, a non-linear LSA is conducted to simultaneously refine the pose and cylindrical/planar feature parameters by minimizing the sum of squared normal distances between the LiDAR points and their respective parametric models. Figure 9b shows two sample map trees before and after optimization, where the misalignment is reduced.

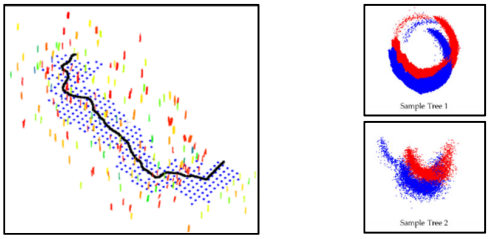

(a) (b)

Figure 9. (a) Mapped trees and ground patches from 1,000 scans (map trees are colored by feature ID, ground patches are colored in blue, and initial trajectory is colored in black) and (b) top view of two sample map trees before (blue) and after (red) map re-optimization.

4. EXPERIMENTAL RESULTS

In this study, the datasets collected at two study sites in the Martell natural forest were used to validate the performance of the proposed frameworks. Specifically, both the F^2-LSLAM and IS^2-TEAM strategies were adopted to process each dataset. To serve as a fair comparison, trajectory information was also used in the F^2-LSLAM strategy. Moreover, the *BP-HM* data were processed using the Emesent Hovermap's post-processing software and used as a reference. The experiment results for study sites 1 and 2 will be presented in this section.

4.1 Experimental Results of Study Site 1

As mentioned in Section 2.2, a reference UAV point cloud is available for this study site. Therefore, the UAV data were used in the process for the three in-house developed backpack datasets. To do so, a preprocessing step was performed to derive DTM and tree locations from the reference UAV point cloud for map initialization. The former was generated through the adaptive cloth simulation algorithm (Lin et al., 2021b) with a resolution of 10 cm, while the latter was derived using the height/density-based tree detection/localization approach proposed by Lin et al. (2021a). In addition, manual DBH measurements for trees whose diameter exceeds 10 cm in the northern part of the covered area are available. The UAV reference point cloud, *BP-HM* data, and manual DBH measurements will be used for analysis.

The assessment of the proposed framework starts by presenting the derived trajectory and extracted tree trunk/ground features in the process. Then, the point cloud is reconstructed using the derived trajectory for each system without performing any noisy-points removal process. Two sample regions of interest (ROIs) over the areas with DBH reference data are extracted for the following analysis:

Point cloud alignment quality: For qualitative analysis, a sample tree is manually segmented from all backpack point clouds for comparison. To perform quantitative evaluation, DBH values of trees in the ROIs are derived from each backpack point cloud. For each tree, the trunk portion in the height range of 1.3–1.5 m above ground is first extracted. An iterative circle fitting process is performed to remove outliers and estimate the diameter (i.e., DBH). Lastly, for trees with reference data, statistics related to DBH residuals will be reported.

Point cloud positional accuracy: Positional accuracy of backpack point clouds is verified against the UAV reference point cloud by visually checking the alignment of a sample tree.

Capability of extracting all tree trunks: An advantage of the proposed frameworks is the ability to extract tree trunk features through the process. To evaluate the performance, the number of trees in the ROIs is manually counted and compared to that extracted from the F^2-LSLAM and IS^2-TEAM strategies for each dataset.

Results from both F^2-LSLAM and IS^2-TEAM strategies for the sample *BP-VLP16HR* dataset are presented in Figure 10, including the derived trajectory and extracted ground/tree trunk feature points. It can be observed that there is no noticeable discontinuity or misalignment between the beginning and end of the mission for both frameworks. For the IS^2-TEAM strategy performing feature extraction from integrated scans, a greater number of features, especially the ground points, were derived in the process. In spite of this, F^2-LSLAM strategy can still derive a reasonable trajectory. Similar findings can be observed for the results from the other two datasets collected using *BP-HDL32* and *BP-VLP16* systems. Next, the qualitative and quantitative assessment of these results are conducted on two square ROIs (with an area of 40 by 40 m), which are highlighted by red boxes in Figure 10a.

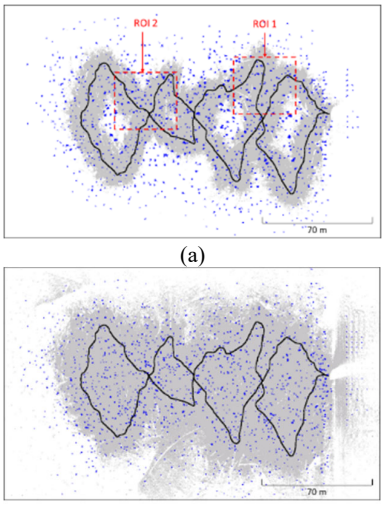

(a)

(b)

Figure 10. Top view of processing results for the *BP-VLP16HR* datasets using (a) F^2-LSLAM and (b) IS^2-TEAM strategies, where the derived trajectory is colored in black, extracted ground points and tree trunk features are colored in gray and blue, respectively.

To evaluate the alignment quality of backpack point clouds, a sample tree from *ROI-2* was manually segmented from each dataset. Figure 11 displays the side view of this tree and a cross section of the tree trunk. Overall, the tree trunks are well-defined in all datasets, with the *BP-HM* point cloud exhibiting the smallest noise level. The alignment quality of IS^2-TEAM results is slightly better than the F^2-LSLAM strategy. The alignment quality is also quantitatively evaluated through DBH estimation. There are 59 and 64 reference DBH measurements in *ROI-1* and *ROI-2*, respectively. Table 2 presents the mean, standard deviation (STD), and RMS of the differences between the estimated DBH values and reference data. It can be observed from the table that F^2-LSLAM and IS^2-TEAM strategies produced comparable results. The mean differences suggest that *BP-VLP16* and *BP-VLP16HR* results tend to underestimate the DBH values, while *BP-HDL32* results overestimate them. Regarding the RMS of the differences, the values of the proposed SLAM strategies are 1-2 cm larger than those of the *BP-HM* results. The qualitative and quantitative evaluations reveal that the proposed frameworks can produce point clouds with reasonable alignment quality from the in-house developed backpack systems for both strategies, and the estimated DBH values have an accuracy of 2-4 cm. However, the alignment quality of the point clouds is not as good as that of the commercial backpack system.

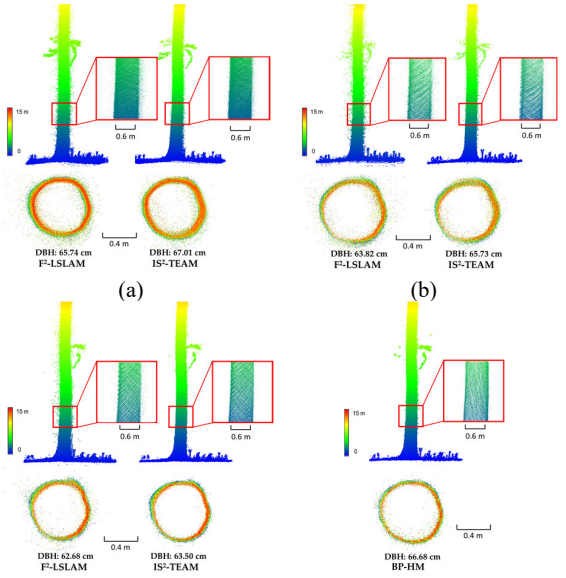

(a) (b)

(c) (d)

Figure 11. A sample tree (with a reference DBH value of 68.32 cm) and the cross section in the height range of 1.3–1.5 m above ground (colored by height) derived from the F^2-LSLAM and IS^2-TEAM results for the in-house developed backpack systems: (a) *BP-HDL32*, (b) *BP-VLP16*, and (c) *BP-VLP16HR*, as well as the (d) *BP-HM* point cloud.

The positional accuracy of the derived point clouds is validated through comparison with the reference UAV point cloud. Figure 12 shows the sample tree from the two in-house developed backpack systems overlaid with the one from UAV. The ground, tree trunk, as well as branches from the in-house developed backpack datasets are in good agreement with the UAV point cloud in all directions, indicating high positional accuracy of the results from both strategies. To evaluate the ability of the proposed frameworks to extract tree trunks, the number of trees within these two ROIs was manually counted from the point clouds of the BP-HDL32 system. There were 84 and 137 trees identified for the two ROIs. Table 3 lists the number of detected tree trunks (N_{DT}), true positives (TP), false positives (FP), and false negatives (FN), as well as the corresponding precision, recall, and F1 score metrics within each ROI for the in-house developed backpack systems using F^2-LSLAM and IS^2-TEAM strategies. The false positives and precision values suggest that the commission errors as represented by the precision metric are low in all cases for the F^2-LSLAM strategy, while the errors are

slightly higher in the IS^2-TEAM strategy. Since the tree density in ROI-2 is higher than that in ROI-1, the omission errors for the former are higher due to the occlusions for the F^2-LSLAM strategy. Additionally, the presence of young and small trees, especially in ROI-2, also contributes to the missing ones. On the other hand, through the feature extraction from integrated scans, the IS^2-TEAM strategy was able to derive more tree trunk features, leading to higher recall values. In summary, the proposed strategy successfully extracts the majority of trees, especially mature ones, in these two regions for all in-house developed backpack systems.

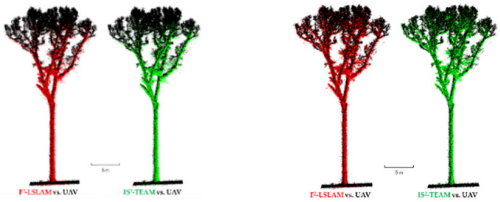

(a) (b)

Figure 12. A sample tree in the (a) *BP-HDL32* and (b) *BP-VLP16HR* point clouds from the F^2-LSLAM (red) and IS^2-TEAM (green) strategies overlaid with the UAV reference point cloud (black).

4.2 Experimental Results of Study Site 2

Different from study site 1, this study site is much more challenging due to the height difference and dense undergrowth vegetation during the data acquisition. Because of this, the F^2-LSLAM strategy could not extract sufficient features from individual scans, leading to the failure of the SLAM process. On the other hand, the IS^2-TEAM strategy exhibited good performance for the *BP-VLP16HR* dataset. Figure 13 shows the IS^2-TEAM results, where ground and tree trunk features were successfully extracted from the integrated scans. The derived trajectory aligns well between the beginning and end of the mission. To evaluate the alignment quality of the IS^2-TEAM results, a sample tree was manually segmented from the *BP-VLP16HR* and *BP-HM* point clouds. Figure 14 displays the side view of this tree and a cross section of the tree trunk. The alignment quality from the proposed framework is reasonable. However, similar to the observations from the results of study site 1, the *BP-HM* provided point clouds with better alignment quality.

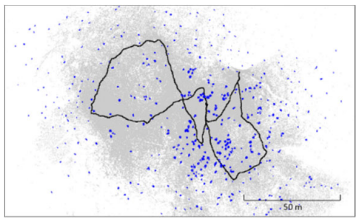

Figure 13. Top view of SLAM results for the *BP-VLP16HR* datasets using IS^2-TEAM strategy, where the derived trajectory is colored in black, extracted ground points and tree trunk features are colored in gray and blue, respectively.

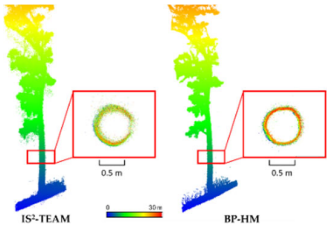

Figure 14. A sample tree and the cross section in the height range of 5.0–6.0 m above ground (colored by height) derived from the IS^2-TEAM results for the *BP-VLP16HR* dataset and the *BP-HM* point cloud.

	Datasets	Number of DBH values	F^2-LSLAM Differences in DBH (cm)			IS^2-TEAM Differences in DBH (cm)		
			Mean	STD	RMS	Mean	STD	RMS
ROI-1	*BP-HDL32*	59	0.81	2.63	2.73	-0.28	1.89	1.90
	BP-VLP16	58	-1.95	3.37	3.87	-1.69	3.08	3.49
	BP-VLP16HR	56	-3.00	2.48	3.88	-2.84	2.15	3.55
	BP-HM	59	-0.30	1.64	1.65	-0.30	1.64	1.65
ROI-2	*BP-HDL32*	64	2.30	2.52	3.40	0.73	2.20	2.30
	BP-VLP16	64	-2.07	2.05	2.90	-1.10	2.05	2.31
	BP-VLP16HR	63	-1.51	2.88	3.23	-1.99	2.74	3.37
	BP-HM	64	-0.07	1.70	1.70	-0.07	1.70	1.70

Table 2. DBH estimation accuracy assessment on backpack point clouds for the two ROIs.

	Datasets	Frameworks	N_{DT}	TP	FN	FP	Precision	Recall	F1 score
ROI-1 (84 trees)	*BP-HDL32*	F^2-LSLAM	81	81	3	0	1.000	0.964	0.982
		IS^2-TEAM	82	80	4	2	0.976	0.952	0.964
	BP-VLP16	F^2-LSLAM	80	79	5	1	0.988	0.940	0.963
		IS^2-TEAM	82	79	5	3	0.963	0.941	0.952
	BP-VLP16HR	F^2-LSLAM	77	76	8	1	0.987	0.905	0.944
		IS^2-TEAM	80	77	7	3	0.963	0.917	0.939
ROI-2 (137 trees)	*BP-HDL32*	F^2-LSLAM	126	125	12	1	0.992	0.912	0.951
		IS^2-TEAM	135	130	7	5	0.963	0.949	0.956
	BP-VLP16	F^2-LSLAM	119	119	18	0	1.000	0.869	0.930
		IS^2-TEAM	135	129	8	6	0.956	0.942	0.949
	BP-VLP16HR	F^2-LSLAM	123	123	14	0	1.000	0.898	0.946
		IS^2-TEAM	136	129	8	7	0.949	0.942	0.945

Table 3. Performance of the tree trunk extraction in the two ROIs from the F^2-LSLAM and IS^2-TEAM results of in-house developed backpack systems.

5. CONCLUSIONS AND RECOMMENDATIONS FOR FUTURE WORK

In this paper, F^2-LSLAM and IS^2-TEAM frameworks are proposed for LiDAR based forest inventory. The F^2-LSLAM strategy consists of two threads: odometry and mapping. The odometry thread extracts semantic features including ground and tree trunks while the mapping thread performs local and global LSA using extracted semantic features to register LiDAR scans to a common reference frame. As for IS^2-TEAM, feature extraction is performed on the integrated scans derived from the GNSS/INS trajectory. Then, the same mapping thread of F^2-LSLAM is utilized to register all integrated scans. These frameworks also support the incorporation of reference point clouds from other sources.

Although it is not as good as the commercial backpack system, reasonable alignment quality was achieved for the in-house developed backpack systems, providing DBH estimates with an accuracy of 2-4 cm in areas with relatively flat terrain and visible tree trunks for both frameworks. The qualitative evaluation revealed that an approximately 10 cm positional accuracy was achieved when reference point cloud was employed in the process. As for the ability to extract tree trunk features, experimental results suggested that the majority of mature tree trunk features were successfully extracted for all systems, with an average F1 score higher than 0.93. However, for more challenging areas with dense undergrowth vegetation and/or large height differences, integrated scan-based feature extraction is more reliable. The main limitation of the proposed frameworks is that the point cloud alignment quality is not as good as the commercial backpack system. More research efforts are needed on incorporating geometric features (e.g., surface elements) and finer semantic features (such as branches) and RGB cameras, in optimizing the SLAM process.

6. ACKNOWLEDGMENT

This work is supported in part by the U.S. Department of the Navy, Cooperative Ecosystem Studies Unit program (Agreement # N400852220004) and the U.S. Department of Agriculture, National Institute of Food and Agriculture, Sustainable Agriculture Systems project (2023-68012-38992).

REFERENCES

Barbeito, I., Dassot, M., Bayer, D., Collet, C., Drössler, L., Löf, M., del Rio, M., Ruiz-Peinado, R., Forrester, D.I., Bravo-Oviedo, A., Pretzsch, H., 2017. Terrestrial laser scanning reveals differences in crown structure of Fagus sylvatica in mixed vs. pure European forests. For Ecol Manage 405, 381–390.

Chen, S.W., Nardari, G. v, Lee, E.S., Qu, C., Liu, X., Romero, R.A.F., Kumar, V., 2020. SLOAM: Semantic LiDAR odometry and mapping for forest inventory. IEEE Robot Autom Lett 5, 612–619.

Corte, A.P.D., Rex, F.E., de Almeida, D.R.A., Sanquetta, C.R., Silva, C.A., Moura, M.M., Wilkinson, B., Zambrano, A.M.A., da Cunha Neto, E.M., Veras, H.F.P., de Moraes, A., Klauberg, C., Mohan, M., Cardil, A., Broadbent, E.N., 2020. Measuring individual tree diameter and height using gatoreye high-density UAV-LiDAR in an integrated crop-livestock-forest system. Remote Sens (Basel) 12.

Goodbody, T.R.H., Coops, N.C., White, J.C., 2019. Digital Aerial Photogrammetry for Updating Area-Based Forest Inventories: A Review of Opportunities, Challenges, and Future Directions. Current Forestry Reports 55–75.

Hartley, R.J.L., Jayathunga, S., Massam, P.D., de Silva, D., Estarija, H.J., Davidson, S.J., Wuraola, A., Pearse, G.D., 2022. Assessing the Potential of Backpack-Mounted Mobile Laser Scanning Systems for Tree Phenotyping. Remote Sens (Basel) 14.

Hyyppä, E., Yu, X., Kaartinen, H., Hakala, T., Kukko, A., Vastaranta, M., Hyyppä, J., 2020. Comparison of Backpack, Handheld, Under-Canopy UAV, and Above-Canopy UAV Laser Scanning for Field Reference Data Collection in Boreal Forests. Remote Sens (Basel) 12, 3327.

Kangas, A., Maltamo, M., 2006. Forest Inventory. Methodology and Applications, Managing Forest Ecosystems.

Khosravipour, A., Skidmore, A.K., Isenburg, M., Wang, T., Hussin, Y.A., 2014. Generating pit-free canopy height models from airborne LiDAR. Photogramm Eng Remote Sensing 80, 863–872.

Kukko, A., Kaijaluoto, R., Kaartinen, H., Lehtola, V. V, Jaakkola, A., Hyyppä, J., 2017. Graph SLAM correction for single scanner MLS forest data under boreal forest canopy. ISPRS Journal of Photogrammetry and Remote Sensing 132, 199–209.

Lin, Y.C., Liu, J., Fei, S., Habib, A., 2021a. Leaf-off and leaf-on uav lidar surveys for single-tree inventory in forest plantations. Drones 5.

Lin, Y.C., Manish, R., Bullock, D., Habib, A., 2021b. Comparative analysis of different mobile LiDAR mapping systems for ditch line characterization. Remote Sens (Basel) 13.

Miller, Z.M., Hupy, J., Chandrasekaran, A., Shao, G., Fei, S., 2021. Application of Postprocessing Kinematic Methods with UAS Remote Sensing in Forest Ecosystems. J For 1–13.

Pierzchała, M., Giguère, P., Astrup, R., 2018. Mapping forests using an unmanned ground vehicle with 3D LiDAR and graph-SLAM. Comput Electron Agric 145.

Sofia, S., Sferlazza, S., Mariottini, A., Niccolini, M., Coppi, T., Miozzo, M., la Mantia, T., Maetzke, F., 2021. A case study of the application of hand-held mobile laser scanning in the planning of an italian forest (Alpe di Catenaia, Tuscany), in: International Archives of the Photogrammetry, Remote Sensing and Spatial Information Sciences - ISPRS Archives.

Su, Y., Guo, Q., Jin, S., Guan, H., Sun, X., Ma, Q., Hu, T., Wang, R., Li, Y., 2020. The Development and Evaluation of a Backpack LiDAR System for Accurate and Efficient Forest Inventory. IEEE Geoscience and Remote Sensing Letters.

Tang, J., Chen, Y., Kukko, A., Kaartinen, H., Jaakkola, A., Khoramshahi, E., Hakala, T., Hyyppä, J., Holopainen, M., Hyyppä, H., 2015. SLAM-aided stem mapping for forest inventory with small-footprint mobile LiDAR. Forests 6.

Xie, Y., Yang, T., Wang, X., Chen, X., Pang, S., Hu, J., Wang, A., Chen, L., Shen, Z., 2022. Applying a Portable Backpack Lidar to Measure and Locate Trees in a Nature Forest Plot: Accuracy and Error Analyses. Remote Sens (Basel) 14.

Zhou, T., Ravi, R., Lin, Y.C., Manish, R., Fei, S., Habib, A., 2023. In Situ Calibration and Trajectory Enhancement of UAV and Backpack LiDAR Systems for Fine-Resolution Forest Inventory. Remote Sens (Basel) 15.